Keeping 2D Materials Visible Even Buried in SoI Wafers

Ergun Simsek* and Bablu Mukherjee
Department of Electrical and Computer Engineering, The George Washington University,
Washington, D.C. 20052, USA

ABSTRACT

In order to protect optoelectronic and mechanical properties of atomically thin layered materials (ATLMs) fabricated over SiO_2/Si substrates, a secondary oxide or nitride layer can be capped over. However, such protective capping might decrease ATLMs' visibility dramatically. Similar to the early studies conducted for graphene, we numerically determine optimum thicknesses both for capping and underlying oxide layers for strongest visibility of monolayer MoS_2, $MoSe_2$, WS_2, and WSe_2 in different regions of visible spectrum. We find that the capping layer should not be thicker than 60 nm. Furthermore the optimum capping layer thickness value can be calculated as a function of underlying oxide thickness, and vice versa.

Keywords: 2D Layered Materials, Nanosheets, Reflectivity, Optical Contrast

1. INTRODUCTION

Graphene [1, 2] and its successors, atomically thin transition metal dichalcogenides (TMDs) [3-7], have received a growing attention due to their remarkable optical, electronic, and mechanical properties. They are considered as one of the main ingredients of next generation opto-electronic technologies. Despite this great interest, the field of 2D materials is still immature. Especially for TMDs, there is still a lack of theoretical frameworks that can fully explain how TMD excitons are affected by temperature, doping level, or substrate changes. Researchers have been carrying out different types of experiments such as optical, Raman, and two-photon spectroscopy to understand the complex physics behind their extremely dispersive nature. Engineers have been trying to fabricate and test TMD based opto-electronic devices such as transistors. Both for fundamental studies and advanced studies, mono- and a few- layers of TMDs are generally deposited on top of either silicon or sapphire substrates via mechanical exfoliation or chemical vapor decomposition. However, these one atom thick layers are not easy to see even with a microscope. In order to make them more visible and easy to work with, Blake *et al.* [1] first calculated the optimum oxide thickness values for silicon wafers and then they confirmed their theoretical results with experiments. Since then the ranges of 90-95 nm and 270-300 nm have become industry standards thanks to constructive and deconstructive interferences occurring in those dimensions that maximize graphene's visibility. Later, the same group conducted new set of experiments on thin TMD films and found out that those two ranges can be used for thin film TMD applications as well [2].

Graphene and other atomically thin layered materials all have exciting features but at the same time they are highly vulnerable and their optoelectronic properties might be damaged easily with environmental factors such as dirt, heat, humidity and gaseous environment containing O_2^- ion and H_2O molecules etc. One possible solution is covering them with a thin oxide or nitride layer. However, such additional layer might decrease their visibility dramatically.

In this work, we numerically calculate the visibility of graphene and four commonly studied TMDs (namely MoS_2, $MoSe_2$, WS_2, and WSe_2) placed between two oxide layers. We find that the capping layer should not be thicker than 60 nm. Furthermore, we derive some analytical equations where the thickness of the capping layer can be calculated as a function of underlying oxide layer thickness (or vice versa) for the highest possible visibility under white, green, and red light. The current industry standards (~95 nm and ~285 nm for the underlying oxide thickness) might be still used for red light illumination, but thinner oxides should be used for white and green light illuminations.

* E-mail: simsek@gwu.edu

Silicon Photonics XI, edited by Graham T. Reed, Andrew P. Knights, Proc. of SPIE Vol. 9752, 97520R
© 2016 SPIE · CCC code: 0277-786X/16/$18
· doi: 10.1117/12.2213085

Downloaded From: http://proceedings.spiedigitallibrary.org/ on 06/21/2016 Terms of Use: http://spiedigitallibrary.org/ss/TermsOfUse.aspx

2. THEORY

Figure 1 (a) shows a typical SiO_2/Si substrate, where the oxide thickness is d_{ox}. In Fig. 1 (b), an atomically thin layered material (ATLM) is buried in the oxide layer, where d_1 and d_2 represent the thicknesses of the regions under and over the ATLM, such that $d_{ox} = d_1 + d_2$. We first calculate the reflectance from both structures as a function of wavelength, and then we calculate the contrast *(C)* using the following formula

$$C(\lambda_i) = \frac{R_{ref}(\lambda_i) - R(\lambda_i)}{R_{ref}(\lambda_i)}, \quad (1)$$

where λ_i is the ith wavelength sample chosen over a finite range between λ_{min} and λ_{max}, such that $\lambda_i = \lambda_{min} + (i-1)(\lambda_{max}-\lambda_{min})/(N-1)$ and $i = 1, 2, 3, \ldots, N$. In other words, the contrast is defined as the change in the relative intensity of reflected light in the presence (R) and absence (R_{ref}) of the ATLM. The importance of working with finite ranges and the logic behind the discretization of these ranges will be explained later.

Since the plane wave propagation in a multilayered medium is a very well-known and studied subject, here we do not provide the formulation. One can choose among various methods such as transfer matrix or transmission line network method, which are explained in several optics and electromagnetics books (i.e. [31]) to calculate the reflectance of these substrates. Briefly, we enforce the boundary conditions for transverse-electric and transverse-magnetic fields on the interfaces between each layer, which is described with its complex electrical permittivity, magnetic permeability, and thickness. With the help of Snell's law, we determine the magnitudes of forward (incident and transmitted) and backward (reflected) components for electric and magnetic fields in each layer, iteratively.

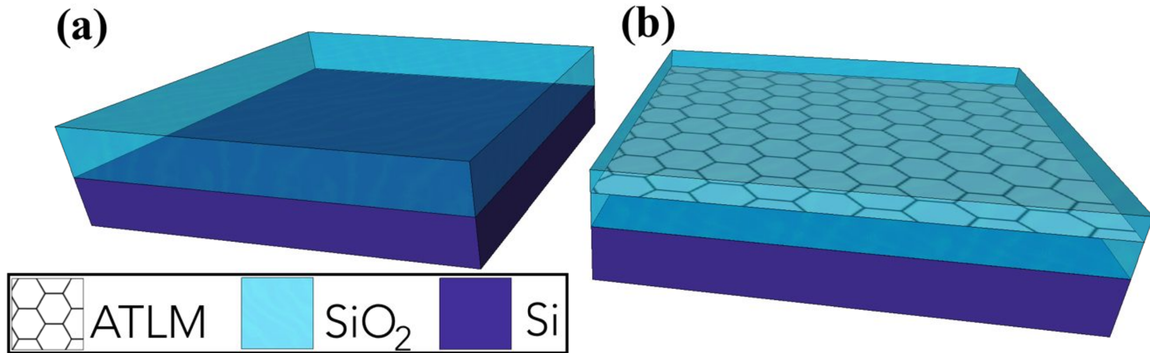

Figure 1 (a) Schematic of a SiO_2/Si wafer, where the thickness of the SiO_2 layer is d_{ox} and (b) an atomically thin layered material is buried in the oxide layer. The thickness of the region between the Si and 2D material is d_1 and the thickness of the upper region is d_2, such that $d_{ox} = d_1 + d_2$.

An important detail is the realistic modeling of materials. In this direction, use wavelength-dependent refractive index formulas for each material. For graphene, the closed form expression developed in [4] is used, assuming room temperature and a hopping parameter of 2.7 eV. The refractive index of MoS_2 is taken from [5]; refractive indices of $MoSe_2$, WS_2, and WSe_2 are taken from [6]. For MoS_2, we assume room temperature and zero Fermi energy. The indices for Si and SiO_2 are taken from [29] and [30], respectively. The thickness of graphene is assumed to be 0.335 nm, whereas monolayer transition metal dichalcogenides are assumed to be 0.7 nm thick.

Downloaded From: http://proceedings.spiedigitallibrary.org/ on 06/21/2016 Terms of Use: http://spiedigitallibrary.org/ss/TermsOfUse.aspx

3. NUMERICAL RESULTS

Before we analyze ATLMs buried in the oxide layer, we study graphene coated SiO_2/Si substrates to verify our implementation and evaluate how much difference occurs when we define graphene as a dispersive material. In [1], the researchers used a constant refractive index value for the definition of graphene over the entire visible spectrum. Here we first use the exact value they used and reproduce their results. Then we recalculate the contrast using the complex electrical permittivity for graphene that changes as a function of wavelength, temperature, and Fermi energy by following the recipe provided in [4]. As shown in Figure 2 (a), our calculations suggest slightly different oxide thicknesses when we use this changing permittivity: the optimum SiO_2 thickness values are 95 nm for white light; 85 nm and 255 nm for green light region; and 100 nm and 305 nm for red light region. Considering the fact that they use constant refractive indices over the entire spectrum and here we fully take dispersion into account (not only for graphene but also for SiO_2 and Si), such difference is not surprising.

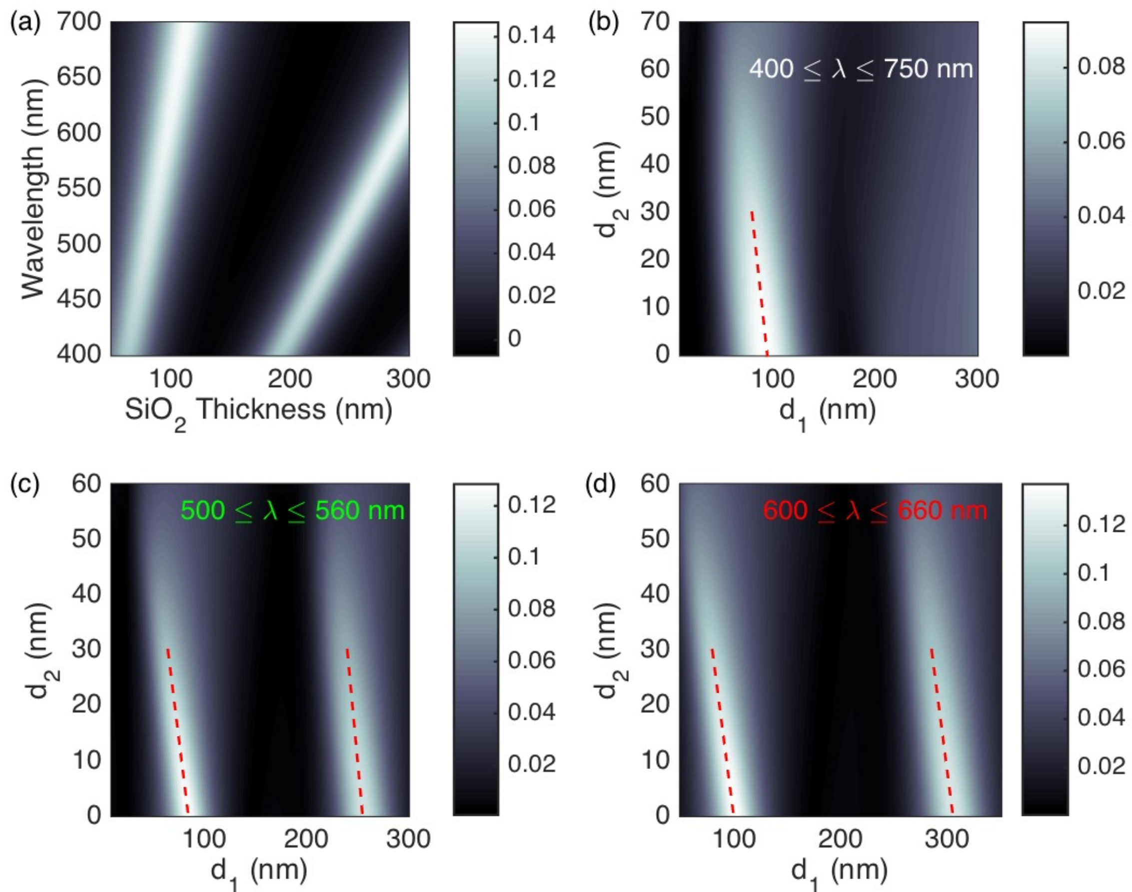

Figure 2 (a) Contrast for graphene coated SiO_2/Si substrate as a function of oxide thickness and wavelength. (b)-(d) Contrasts for graphene buried in the oxide that sits on silicon as a function of d_1 and d_2, thicknesses of the oxide regions below and above the graphene for white, green, and red lights, respectively.

After validating our implementation, we focus on the main subject of our interest: the visibility of ATLMs when buried inside the oxide layer. We treat the substrate as a 4 layer geometry which forms a wave propagation problem in 5 layer medium, from bottom to the top: silicon / oxide / ATLM / oxide / air. In this configuration the top and bottom layers are

Downloaded From: http://proceedings.spiedigitallibrary.org/ on 06/21/2016 Terms of Use: http://spiedigitallibrary.org/ss/TermsOfUse.aspx

infinitely long and the thickness of the inner layers are d_1, 0.7 nm, and d_2, respectively. In order to find the optimum d_1 and d_2 values, we calculate the average contrast (C_{ave}) using the following equation

$$C_{ave} = \frac{1}{N}\sum_{i=1}^{N} C(\lambda_i). \tag{2}$$

We first consider a broadband illumination, which is more applicable for practical applications with standard color cameras avoiding the need for additional color filters, and we calculate the average contrast over the whole visible range, i.e. λ_{min} = 400 nm, λ_{max} = 750 nm, and N = 351. The first thing we notice is that the thickness of the protection SiO_2 layer (d_2) should be smaller than 30 nm and the thickness of the oxide layer between the ATLM and silicon (d_1) should not be bigger than 95 nm and less than 80 nm to have strong visibility. For this case, i.e. d_2 is less than 30 nm and $80 \leq d_1 \leq 95$ nm; we observe a linear trend, which can be written as $d_1 \approx 95\text{-}0.5d_2$. This means that we can systematically choose the optimum oxide thickness values for a certain technology. For example, if the minimum oxide thickness that one can produce is 10 nm, then they should simply choose d_1 = 90 nm and d_2 = 10 nm for the maximum visibility while protecting the graphene from external factors.

We follow the same methodology for shorter ranges (i.e. green $500 \leq \lambda \leq 560$ nm and red $600 \leq \lambda \leq 660$ nm) to mimic the experiments conducted with filtered light. As shown in Figure 2 (c) and (d), there is a secondary region of (d_1, d_2) for good contrast. In this region, d_1 values are much higher (>240 nm) while d_2 still has to be less than or equal to 30 nm. In both regions, the bright spots in each figure of color contrast suggest that an optimum d_1 values can be calculated with the equation (3) as follows:

$$d_1 = \alpha d_2 + \beta, \tag{3}$$

where α is the slope of the dashed line passing through the bright spots and β is a positive number, which can be extracted from the figures of color contrast. For green light ($500 \leq \lambda \leq 560$ nm) region 1: $65 \leq d_1 \leq 85$ nm and $d_1 \approx 85\text{-}0.67d_2$; region 2: $240 \leq d_1 \leq 255$ nm and $d_1 \approx 255\text{-}0.5d_2$. The reason for not having the secondary region for white light illumination is that the contrast values coming from the 400-500 nm and 650-750 nm regions "almost" cancel each other.

To analyze monolayer transition metal dichalcogenides (MoS_2, $MoSe_2$, WS_2 and WSe_2) buried in SiO_2 in sandwich geometry, we employ the same method and obtain similar results. However, we should explain one detail. As discussed in [7], one can find several different permittivity models in the recent literature (e.g. [5] and [6]). Even though they might produce completely different permittivity numbers at a given wavelength, their trend is almost the same. They all show 3 main oscillations in the visible range corresponding to exciton A, exciton B, and the band gap. So this is why such different permittivity models give similar d_1 and d_2 values for the maximum visibility.

Table 1 provides the list of suggested thickness ranges and equations to calculate optimum values for maximum visibility of monolayers of MoS_2, $MoSe_2$, WS_2 and WSe_2 under white, green, and red light excitations. As a rule of thumb, our calculations suggest having (i) a capping oxide layer of 40 nm or less thickness while (ii) the underlying oxide should 40 nm or thicker. The optimum values can be calculated using the formulas provided in the table. The details of this study can be found in [7] that might be useful as benchmark and guideline of oxide/ATLM/oxide sandwich structure for both fundamental studies and device applications at different wavelength regions of solar spectrum.

Note that a very recent and exciting study of Kang *et al.* has shown that it is possible to fabricate vertical stacks of MoS_2/SiO_2 on fused Si substrates. Such structures' optical properties can be studied with the aforementioned wave propagation in layered media methods. In this direction, we calculate the absorptance of single-, double- and triple- unit of monolayer MoS_2/SiO_2 stacks placed on top of silicon substrates. The Fermi energy dependent refractive index of MoS_2 is calculated with the recipe provided in [5] assuming a Fermi energy level of 0.053 eV and room temperature. As shown in Fig. 3 (a), theoretically we have obtained average absorption of ~ 2.6 %, ~5.3 % and ~7.8 % from single, double and triple Bragg stack geometry, respectively. The experimental results [8] report that the average absorption values are ~2.7 %, ~5.4 % and ~8.4 % for single, double and triple vertical stacks, respectively, in wavelength range of 425-725 nm. This good agreement between theoretical and experimental results and the fact that the absorption increases with increasing stack number show us that we can design Bragg stack-like geometries composed of periodic oxide/TMD stacks that can be used as broadband and "ohmic loss free" absorbers. At the conference, we will discuss the limits of such excitonic absorbers in terms of average absorption, bandwidth, and size.

Downloaded From: http://proceedings.spiedigitallibrary.org/ on 06/21/2016 Terms of Use: http://spiedigitallibrary.org/ss/TermsOfUse.aspx

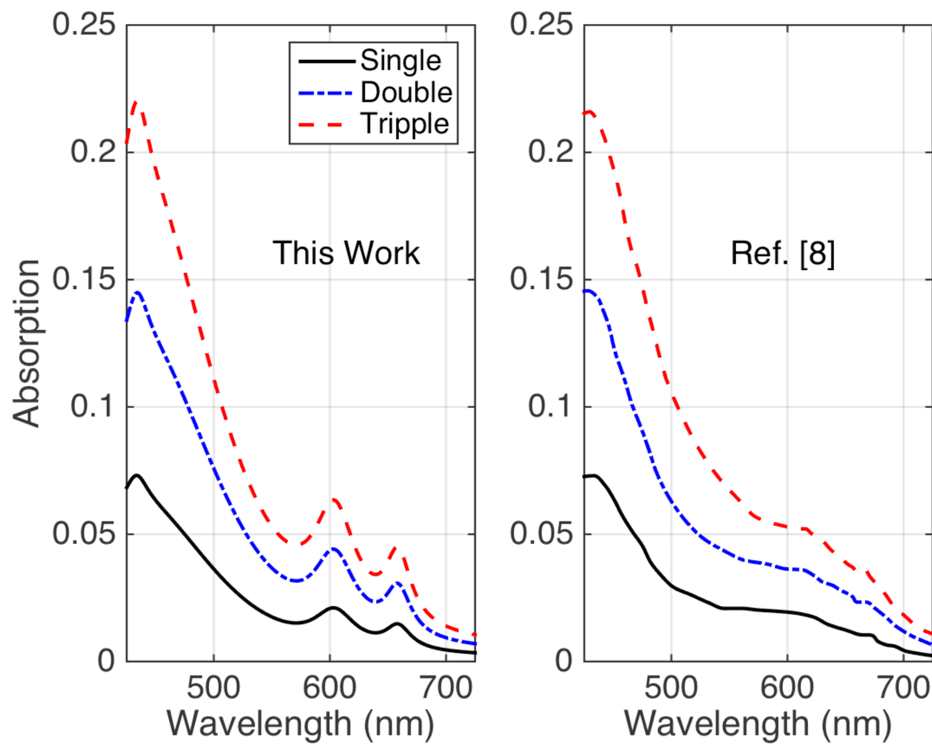

Figure 3 Optical absorption spectra calculated numerically for single-, double- and triple- unit of monolayer MoS_2/SiO_2 in wavelength range of 425-725 nm and (b) as reported experimentally in reference [8].

Table 1. Suggested d_1 ranges and equations to calculate the optimum d_2 values that maximize the visibility of ATLMs over three different wavelength ranges.

	White Light **$400 \leq \lambda \leq 750$ nm** $0 \leq d_2 \leq 50$ nm	**Green Light** **$500 \leq \lambda \leq 560$ nm** $0 \leq d_2 \leq 40$ nm		**Red Light** **$600 \leq \lambda \leq 660$ nm** $0 \leq d_2 \leq 60$ nm	
MoS_2	$d_1 \approx 69-0.44d_2$ $47 \leq d_1 \leq 69$ nm	$d_1 \approx 70-0.675d_2$ $43 \leq d_1 \leq 70$ nm	$d_1 \approx 238-0.6d_2$ $214 \leq d_1 \leq 238$ nm	$d_1 \approx 87-0.683d_2$ $46 \leq d_1 \leq 87$ nm	$d_1 \approx 289-0.63d_2$ $251 \leq d_1 \leq 289$ nm
$MoSe_2$	$d_1 \approx 76-0.52d_2$ $50 \leq d_1 \leq 76$ nm	$d_1 \approx 74-0.675d_2$ $47 \leq d_1 \leq 74$ nm	$d_1 \approx 243-0.6d_2$ $219 \leq d_1 \leq 243$ nm	$d_1 \approx 86-0.7d_2$ $44 \leq d_1 \leq 86$ nm	$d_1 \approx 287-0.63d_2$ $249 \leq d_1 \leq 287$ nm
WS_2	$d_1 \approx 68-0.5d_2$ $43 \leq d_1 \leq 68$ nm	$d_1 \approx 71-0.7d_2$ $43 \leq d_1 \leq 71$ nm	$d_1 \approx 239-0.625d_2$ $214 \leq d_1 \leq 239$ nm	$d_1 \approx 85-0.683d_2$ $44 \leq d_1 \leq 85$ nm	$d_1 \approx 288-0.67d_2$ $248 \leq d_1 \leq 288$ nm
WSe_2	$d_1 \approx 71-0.52d_2$ $45 \leq d_1 \leq 71$ nm	$d_1 \approx 73-0.7d_2$ $45 \leq d_1 \leq 73$ nm	$d_1 \approx 241-0.625d_2$ $216 \leq d_1 \leq 241$ nm	$d_1 \approx 83-0.7d_2$ $41 \leq d_1 \leq 83$ nm	$d_1 \approx 284-0.65d_2$ $245 \leq d_1 \leq 284$ nm

Downloaded From: http://proceedings.spiedigitallibrary.org/ on 06/21/2016 Terms of Use: http://spiedigitallibrary.org/ss/TermsOfUse.aspx

4. DISCUSSIONS

Equation (2) gives us the average contrast assuming the intensity of light is constant over the entire spectrum, which is not the case in real life. In order to take the wavelength dependent intensity of our broadband source (Ocean Optics HL-2000 tungsten halogen bulb) into account, we repeat the same calculations using the following formula

$$C^*_{ave} = \frac{\sum_{i=1}^{N} I_i C(\lambda_i)}{\sum_{i=1}^{N} I_i}. \quad (4)$$

where I_i is the relative intensity of the light, which is calculated through a simple interpolation at the ith discrete wavelength sample. The data of the spectral output is downloaded from Ocean Optics' website (http://oceanoptics.com). Interestingly, the change in the average contrast was so small (less than 1-2 %).

5. CONCLUSION

Optical, electronic, and mechanical properties of atomically thin layered materials can be protected by covering them with oxide or nitride thin films. In this work, we have numerically investigated the visibility of graphene and monolayers of transition metal dichalcogenides when they are protected with oxide thin films. Our calculations show that the thickness of the protection layer should be less than or equal to 50, 40, and 60 nm for white, green, and red lights, respectively. Furthermore the thickness of the underlying oxide can be calculated as a function of protection layer thickness for a chosen wavelength range.

REFERENCES

[1] Blake P., Hill E. W., Castro Neto A. H., Novoselov K. S., Jiang D., Yang R., Booth T. J., and Geim A. K., "Making graphene visible," Appl. Phys. Lett. 91, 063124, (2007).

[2] Simsek E., "A Closed-Form Approximate Expression for the Optical Conductivity of Graphene," Optics Letters 38(9), 1437-1439, (2013).

[3] Benameur M. M., Radisavljevic B., Sahoo S., Berger H., and Kis A., "Visibility of dichalcogenide nanolayers," Nanotechnology 22, 125706 (2011).

[4] Lien D. H., Kang J. S., Amani M., Chen K., Tosun M., Wang H. P., Roy T., Eggleston M. S., Wu M. C., Dubey M., Lee S-C., He J-H., Javey A., "Engineering Light Outcoupling in 2D Materials," Nano Lett. 15(2), 1356-1361 (2015).

[5] Mukherjee B., Tseng F., Gunlycke D., Amara K. K., Eda G., Simsek E., "Complex Electrical Permittivity of the Monolayer Molybdenum Disulfide (MoS_2) in Near UV and Visible," Opt. Mat. Exp. 5(2), 447-455, (2015).

[6] Li Y., Chernikov A., Zhang X., Rigosi A., Hill H. M., van der Zande A. M., Chenet D. A., Shih E., Hone J., Heinz T. F. "Measurement of the optical dielectric function of monolayer transition-metal dichalcogenides: MoS_2, $MoSe_2$, WS_2, and WSe_2," Phys. Rev. B 90, 205422 (2014).

[7] Simsek E., Mukherjee B., "Visibility of Atomically Thin Layered Materials Buried in Silicon Dioxide," IOP Nanotechnology 26 (45), 455701 (2015).

[8] Kang K., Xie S., Huang L., Han Y., Huang P. Y., Fai Mak K., Kim C. J., Muller D., Park J., "High-mobility three-atom-thick semiconducting films with wafer-scale homogeneity," Nature 520, 656 (2015).

Downloaded From: http://proceedings.spiedigitallibrary.org/ on 06/21/2016 Terms of Use: http://spiedigitallibrary.org/ss/TermsOfUse.aspx